JJEES

Volume 1, Number 2, December. 2008
ISSN 1995-6681
Pages 53-62

Jordan Journal of Earth and Environmental Sciences

Geochemistry, Mineralogy and Petrogenesis of El-Lajjoun Pleistocene Alkali Basalt of Central Jordan.

Tayel El-Hasan *[a] and Ahmad Al-Malabeh [b]

[a] Faculty of science, Mu'tah University , Al-Karak, Jordan,

[b] Department of Earth and Environmental Science, the Hashemite,University, Zarka, Jordan.

Abstract

The El-Lajjoun basalt (hereafter, LB) is a Wadi-fill flow that covers an area of about 10 km^2 in Central Jordan. The tectonic evaluation carried out through lineament and fracture analyses indicates that the regional development is tectonically related to the opening of the Red Sea, and the development of the Dead Sea transform fault and other distinct regional tectonic features. The age of the LB (middle Pleistocene) can be correlated with the second stage of the opening of the Red Sea over the last 5 Ma. Petrographic data shows that rocks are plagioclase, olivine, pyroxene, and magnetite-phyric basalts. They correspond to alkali olivine basalts and basanites. The LB rocks are very similar in composition, and have comparable ranges of major and trace element concentrations. They are of undersatured silica type and belong to sodic to mildly alkaline magma series. The distinctive geochemical characteristics of LB indicated that LB was derived from a slightly fractionated magma as reflected by its high MgO (7-8 wt%) concentration, the Mg-number (0.60-0.63), the low silica content (<43-46 wt%), and the relatively high Ni and Cr concentrations (193-271 ppm and 243-374 ppm, respectively). This basalt is resulted from a low degree of partial melting (10%) of a homogeneous garnet peridotite mantle source in the asthenosphere at a depth > 100 km.

Keywords: Pleistocene, Alkali-olivine basalt, Within-plate basalt, Partial melting

1. Introduction

The tectonic evolution of the Arabian plate is determined by the main regional structures of the region including the African Arabian rift system, the collision of the Arabian and Eurasian plates, and the Arabian dome (Barberi et al. 1970; Almond, 1986; Garfunkel, 1988; Burke, 1996; and Al-Malabeh et al. 2004) (Figure 1). This evolution led to different fractures and rifting systems, i.e. the East-African rift, the opening of the Red Sea, and the Dead Sea rift system. These tectonics were controlling the volcanic activity in the Arabian plate which are sporadically found over an area that covers a distance of 7,000 Km from Yemen in the south through Saudi Arabia, Jordan, Syria, and up to Turkey in the north (Coleman and McGuire 1988; Camp and Roobol 1992; and Pick et al. 1999).

The basaltic rocks in Jordan are mainly of Tertiary - Quaternary in age. They occupy 18 % of Jordan's area; and are distributed in three main regions based on their mode of occurrences according to (Bender, 1974; and Al-Malabeh, 1993): 1) within Jordan rift (e.g. Zara basalt), 2) central Jordan (e.g. El-Lajjun basalt) and 3) NE-Jordanian Harrat (with an area 11,400 km^2) which is a part of the largest Harrat Al-Shaam (Al-Malabeh, 2003) as shown in (Figure 2a).

Based on K-Ar, Barbari et al. 1979; Moffat, 1988 ; Duffield et al. 1988; and Ilani et al. 2001 have divided the volcanic activity of Jordan into three major episodes: Oligocene to early Miocene (26.23-22.17 Ma), middle to late Miocene (13.97-8.94 Ma), and late Miocene to Pleistocene (6.95 Ma to < 0.15 Ma). Previous petrochemical studies of basaltic rocks indicated that NE basaltic plateau is composed of alkali basalts and basanites with minor nephelinites (e.g. Barberi et al. 1979; Moffat, 1988; Saffarini et al. 1985; Al-Malabeh, 1994; Al-Malabeh et al. 2002; Shaw et. al. 2003; Ibrahim and Al-Malabeh 2006).

The basalt in central Jordan, which is of our concern here, is found mainly in six places, namely El-Lajjoun, Jabal Shihan, Tafila, Wadi Dana, Jurf Al-Darawish and Ghor Al-Katar. They occur either as plateau basalts, or as local flows, (e.g., Wadi fills) or as individual volcanic bodies (cones, plugs, sills, and dikes). In spite of the fact that substantial horizontal sinistral displacement of N-S striking the Dead Sea Transform Fault (DST) is accompanied by sinistral fan-like rotation of the Arabian plate., this might have led to the opening of fissures for the ascent of magmas. The available geochronological data for these basalts suggests a different story. The several doleritic dikes along the NW-SE Al-Karak - Wadi Al-Fayha fault zone (graben) with the an age of 28.8- 18.9 Ma belong to the oldest phase of activity, whereas the ages of activities in the other sites are more recent; such as in Wadi Dana 9.3 – 5.1 Ma (Steinitz and Batrov, 1992); in Shihan plateau 6.0 Ma (Barberi et al. 1979) and in Tafila

* Corresponding author.; tayel@mutah.edu.jo

3.7 -1.7 Ma (Steinitz and Batrov, 1992). Therefore, the association of theses basalts only with the DST is questionable since some of them are dated older than the rift. Therefore it is better to relate them to the development of the Arabian plate, coeval on a large scale with the regional uplifting, and with rifting phases (Garfunkel, 1989).

This work aims at investigating the geochemical, mineralogical, and petrographical features of the Neogene-Quaternary intra-continental basaltic flows at El-Lajjoun area - central Jordan. And to determine their origin and type of parental magma, and to investigate their relationship to the tectonic evolution of the whole region.

2. Study Area Settings

The LB is located about 15 km east of Al-Karak city at 31°13'40"N and 35°51'52"E (Figure 2a). The flow covers an area of about 10 km^2; and it forms an NE-SW striking, arc-like strip with a width of about 0.5 km with an average thickness of 1-3 m. The exposure starts along the sides of Wadi Adir, and then passes through the El-Lajjoun grazing station, and then along the sides of Wadi Al-Dakain (Figure 2b). This basalt belongs to the middle Pleistocene (Bender, 1968; Heimbach & Huseibeh, 1975; and Steinitz and Batrov, 1992). This is in consistence with the second stage of the opening of the Red Sea over the last 5 Ma.

The basalt is seen in the field to cover Al-Hisa Phosphorite Unit of Mastrichitian age (Al-Shawabkeh, 1991; Latiafeh, et al. 2002; and Al-Malabeh et al. 2002); and is covered by fluviatile and lacustrine gravels and soil (Figs. 2b). The lithostratigraphy of El-Lajjoun area is presented in (Figure 2c).

The results of joint and fault measurements are presented as rose diagrams in (Figure 2d). The LB displays two dominant joint directions, namely N-S and E-W and two minor directions, i.e., NW-SE and NE-SW. These directions are coincided with the main regional and local structural directions. The N-S trending fractures are parallel to (DST). The E-W fractures lie parallel to Salwan Fault and perpendicular to DST, Suwaqa normal fault (Hatcher et al. 1981), Zarka Main fault and El-Lajjoun graben. Moreover, the NE-SW trending joints are consistent with the late Pan-African stress pattern as reported by (Bentor, 1985; and Stern, 1985). They suggested that these trends are formed by extensional stresses normal to their direction. Also, this direction is consistent with the Jurf Al-Darawish fault, which has a vertical displacement of at least 100 m, downthrown to the east (Barjous & Mikbel, 1990). The NW-SE trending directions are shown by a number of prominent regional faults such as the Al-Karak - Al-Fayha fault system (graben) and the Wadi Sirhan fault zone, which extends about 325 km in the same direction starting from Saudi Arabia in the south and continuing to the north of Jordan (Bender, 1974) (Figure 2a).

3. Sampling and Analytical Techniques

Twelve representative rock samples from the LB were crushed and powdered using geochemical techniques. Major oxides and trace elements were analysed on fused glass disks at the Geological Institute, University of Wuerzburg, Germany, by multi-channel XRF spectrometry. Powdered samples were dried for two hours at 110 ^oC and ignited in an electric furnace at 100 ^oC for one hour. Ignited samples were then mixed with sodium tetra-borate and fused in crucibles over gas burners for 1-1.5 hours. Melts were poured into a mold creating 32 mm diameter glass disks. Major and trace elements analytical results are given in Table 1. The Loss On Ignition (LOI) was determined by weight lost after melting at 1000 ^oC.

4. Results

4.1. Petrography and Mineralogy

The LB, in hand specimen, is melanocratic, holocrystalline, medium-grained, and porphyritic. Vesicles have an elongated and oval shape and show pahoehoe structure and fragmented ropy chilled surfaces. The flows exhibit uniform petrographical characteristics. Moreover, the main mineral constituents are plagioclase, olivine, pyroxene, and opaque minerals (mainly magnetite). The secondary minerals include iddingsite, calcite, sericite, and serpentine. Common textures occurring in the LB are intergranular, seriatic, subpilotaxitic, glomeroporphyritic, ophitic, sub-ophitic, vesicular and amygdaloidal textures. The calculated CIPW-norm is listed in Table (2).

4.1.1. Plagioclase

Plagioclase occurs in two generations as larger phenocrysts and as small tabular to elongated microlites in the groundmass. The phenocrysts are subhedral laths, from < 0.5 mm up to 6 mm in length and forming about 35-45 vol.% of the rock. The crystals are quite fresh and well developed; and show lamellar twining. The extinction angles on several plagioclase phenocrysts range from 28° to 32°, indicating a labradorite composition (An50-An70) by using the method described by Michel-Levy's (Kerr, 1977). The crystals show intergranular, radiated and sub-pilotaxitic textures. Glomeroporphyritic texture is occasionally present with clusters of up to four crystals. Seritization is observed along borders and along cleavage planes of the crystals as yellow to turbide rims. Albitization of plagioclase is also recorded where Ca-plagioclase is converted to Na-plagioclase, a process caused by the instability of the Ca-plagioclase during weathering.

4.1.2. Olivine

Olivine occurs as phenocrysts and in groundmass. It forms 10-16 vol. % of the rock. The phenocrysts are euhedral to subhedral. They are colourless to pale grey, and range between 0.08 mm and 5 mm in size, displaying seriate texture. Moreover, the crystals occur both as individuals and as glomeroporphyritic aggregates of more than six crystals. Olivine in the groundmass has subhedral to rounded shape. The larger crystals are fractured slightly–to-moderately. Iddingtization is common, particularly along fractures and along edges of the crystals. Some crystals are partially to completely pseudomorphed to dull brown iddingsite. Groundmass olivine is also iddingsitized.

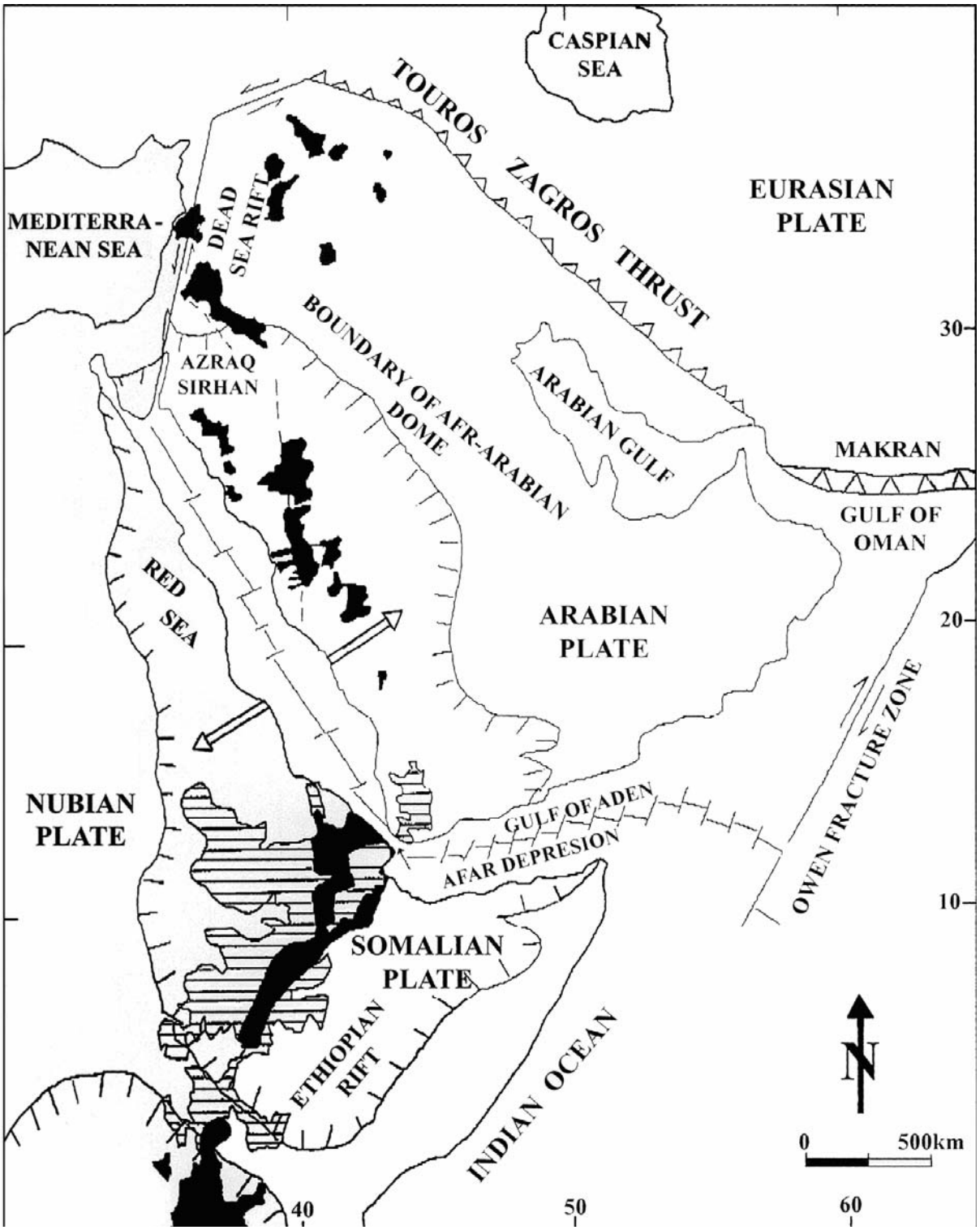

Figure 1: Regional tectonic map of the eastern Mediterranean region and the associated volcanic feature (After *Al-Malabeh, 1993*).

These alteration products are considered to be resulted because of relatively low-temperature deuteric alteration process, or the result of primary olivine oxidation. Due to embayment, Corroded outlines are noticed. Such embayments of olivine crystals were described by (Cox et al. 1979) as a result of interaction between melt and olivine crystals during the crystallization processes. The LB has a normative olivine value that ranges from 14.13 to 19.04 wt %, and averages 15 wt%, which matches the value of modal olivine of 10-16 %. The normative nepheline content ranges between 3.17 and 12.87 wt% (Table 2), which allows classifying the rocks according to criteria of (Le Bas et al. 1986) as alkali olivine basalt and basanite(olv.>10%).

Table 1. Geochemical analytical results of El-Lajjoun basalt (LB), major oxides are in (wt%), trace elements are in (ppm).

Sample#	L1	L2	L3	L4	L5	L6	L7	L8	L9	L10	L11	L12
SiO_2	45.16	43.63	45.01	43.11	45.12	46.52	46.61	45.22	46.34	45.17	45.26	43.85
TiO_2	1.61	1.60	1.63	1.64	1.67	1.66	1.71	1.64	1.76	1.72	1.66	1.68
Al_2O_3	13.45	13.98	14.48	14.92	14.69	14.56	13.42	14.63	13.71	15.07	14.31	14.57
FeOt	12.81	12.68	12.99	12.01	12.12	12.17	11.92	12.11	12.52	12.29	12.46	12.56
MnO	0.16	0.16	0.16	0.16	0.16	0.16	0.17	0.16	0.18	0.16	0.16	0.16
MgO	8.87	8.16	8.78	8.46	8.66	8.84	7.87	8.54	8.30	7.66	8.52	8.41
CaO	11.40	12.94	11.23	12.01	11.98	12.14	11.27	11.78	10.46	11.02	10.68	11.62
Na_2O	2.83	3.35	3.46	3.54	3.45	3.81	3.43	3.33	3.54	3.68	2.92	3.68
K_2O	0.52	0.57	0.60	0.69	0.73	0.67	0.71	0.69	0.68	0.69	0.57	0.69
P_2O_5	0.27	0.26	0.28	0.30	0.29	0.27	0.23	0.31	0.33	0.29	0.41	0.38
LOI	2.68	2.85	2.87	2.14	2.56	1.89	2.01	1.84	1.97	2.13	2.78	2.03
Sum	99.56	99.29	100.20	99.73	99.85	99.62	99.55	100.2	99.74	99.88	99.73	99.63
Mg #	0.62	0.60	0.62	0.63	0.63	0.62	0.62	0.62	0.61	0.63	0.63	0.63
Trace Elements ppm												
Cr	303	319	316	317	320	323	318	234	343	306	291	374
Ni	231	215	230	225	233	227	239	271	265	211	193	214
Sc	21	17	21	23	20	28	22	27	19	21	23	28
Co	59	50	57	54	58	61	52	57	62	51	71	53
V	190	203	196	201	195	213	210	180	195	211	193	214
Sn	14	12	14	13	15	12	14	13	12	16	15	14
Pb	6	6	5	6	5	6	5	6	5	5	6	6
Mo	4	4	4	5	4	6	4	4	5	4	5	5
Sr	727	505	517	546	523	524	520	714	673	571	518	534
Rb	8	10	10	7	9	9	10	9	8	9	7	10
Ba	269	230	199	226	245	255	239	242	262	256	231	259
Zr	103	102	106	104	105	104	107	104	108	107	106	107
Nb	13	13	16	14	13	15	14	13	15	14	15	13
Y	16	17	18	21	20	16	16	20	18	17	17	19
Cr/Ni	1,31	1,48	1,37	1,41	1,37	1,42	1,33	0,86	1,29	1,45	1,5	1,75
Rb/Sr	0,011	0,019	0,019	0,012	0,017	0,017	0,019	0,012	0,012	0,0158	0,013	0,012
Zr/Nb	7,92	7,85	6,62	7,43	8,08	6,93	7,64	8	7,2	7,64	7,067	8,2331
Zr/Y	6,44	6	5,88	4,95	5,25	6,5	6,68	5,2	6	6,29	6,24	5,6347
Y/Nb	1,23	1,31	1,125	1,5	1,54	1,07	1,14	1,54	1,2	1,21	1,133	1,4662

Table 2. CIPW-Norms for El-Lajjoun Basalt (LB).

Sample#	L1	L2	L3	L4	L5	L6	L7	L8	L9	L10	L11	L12
Il	3.06	3.04	3.1	3.12	3.17	3.15	3.25	3.12	3.34	3.27	3.15	3.19
Ap	0.64	0.62	0.66	0.71	0.69	0.64	0.54	0.73	0.78	0.69	0.97	0.9
Or	3.07	3.37	3.55	4.08	4.31	3.96	4.2	4.08	4.02	4.08	3.37	4.08
Ab	14.99	5.85	12.79	6.19	10.48	11.82	18.39	12.21	19.58	14.71	18.86	8.96
An	25.44	21.43	22.21	22.78	22.44	20.65	19.12	22.93	19.51	22.56	24.26	21.2
Di	24.26	33.86	26.11	28.64	28.83	31.05	29.05	27.59	24.96	24.97	21.49	27.99
Mt	4.51	4.49	4.54	4.55	4.6	4.58	4.65	4.55	4.73	4.67	4.58	4.61
Ol	19.04	14.15	18.42	15.59	15.84	15.62	14.13	16.29	17.09	15.69	18.83	16.39
Ne	4.85	12.19	8.93	12.87	10.14	11.06	5.76	8.65	5.62	8.9	3.17	12.01

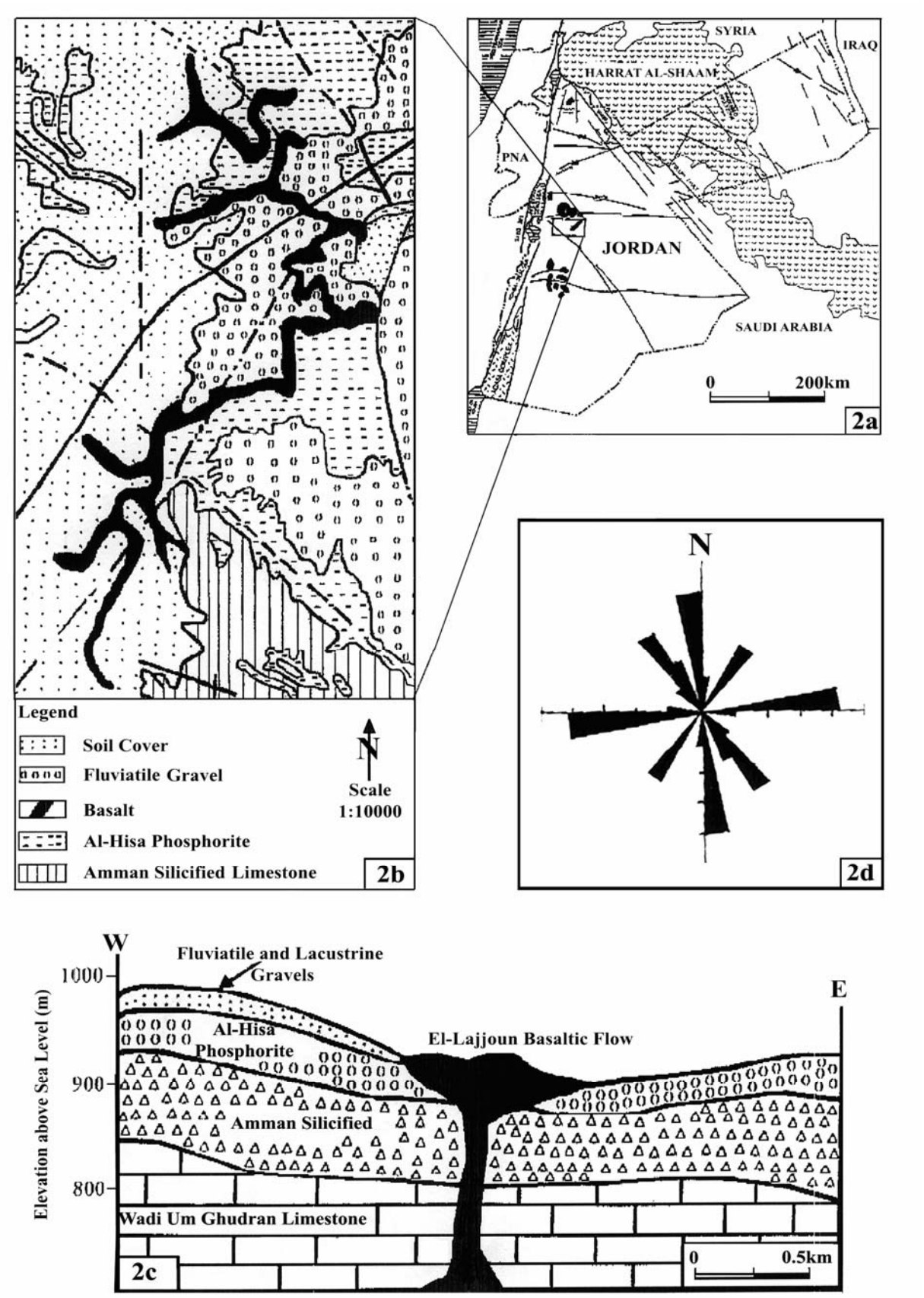

Figure 2: Generalized figure showing: a) Tectonic and volcanic map of Jordan showing the location of the El-Lajjoun basalt (modified after Barjous & Mikbel, 1990; Al-Malabeh, 1993; and Ibrahim, 1996), b) Geologic map of El-Lajjoun basalt and the surrounding area (modified after Al-Shawabkeh, 1991), c) Cross section shows the lithostratigraphy of El-Lajjoun area. d) Rose diagram depicting the orientation pattern of brittle deformation in El-Lajjoun area.

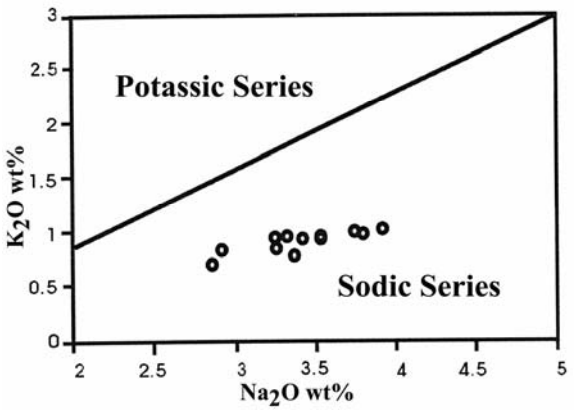

Figure 3: K_2O vs. Na_2O diagram showing the sodic affinity of the LB samples, (*after Middlemost*, 1975).

4.1.3. Pyroxene

Pyroxene occurs as brownish anhedral crystals, forming about 10-15 vol. % of the rock. They show perfect cleavage parallel to [110], and cleavage intersects at ca. 90° in cross sections. The crystals have sizes between 0.3 to 2 mm. These grains exhibit moderately curved fractures. The pyroxene crystals have an inclined extinction of between 49° and 53°, indicating clinopyroxene of augite composition. Pyroxene crystals are affected by chloritization. Green chlorite is present along fractures and along crystal rims. Pyroxene interacts with plagioclase crystals yielding a sub-ophitic texture.

4.1.4. Opaque Minerals

Opaque minerals are common in LB. Opaque minerals range in size from 0.03 mm to 4 mm, forming about 4-6 vol. % of the rock Table (2). They are mostly magnetite phenocrysts scattered throughout the rock and throughout inclusions within olivine and pyroxene crystals. Generally, magnetite is black; and shows homogeneous optical properties. Most of it is anhedral to subhedral, but crystals with square outline are also presented.

4.1.5. Groundmass

The LB groundmass consists mainly of plagioclase (labradorite), olivine, pyroxene (augite) , and opaque minerals (mainly magnetite). Iddingsite, gypsum and calcite are secondary minerals. However, no modal nepheline is recorded.

4.1.6. Vesicles

LB shows spherical to ovoid and elongated vesicles. The long axis ranges from 0.1 to 5 mm. Most of the vesicles are empty, but some are filled with calcite and other secondary minerals (probably gypsum and zeolites). They form about 3-5 vol. % of the rock.

4.2. Rock Geochemistry

4.2.1. Major oxides

The contents of major oxides are in weight percentage, and trace elements are in ppm, listed in Table (1). All samples are very similar in composition. This is evident from the very narrow ranges of major and trace element concentrations. This is mainly illustrated by the narrow range in silica content between 43.63 and 46.61 wt% with an average of 45.08 wt%. This content falls within the averages reported for alkali olivine basalt and basanite by many authors (e.g. Barberi et al. 1979; Cebria and Lopez-Ruiz, 1995; Ibrahim and Al-Malabeh, 2006) and is demonstrated by the nomatiline nepheline.

The MgO content of LB ranges from 7.66 to 8.87 wt% with an average 8.42 wt%. The Mg-number (Mg#), which is defined by Jenner et al. 1987; and Downes et al. 1995, as the molecular proportion of $Mg^{2+}/(Mg^{2+}+Fe^{2+})$ is usually used as a petrogenetic indicator for magma fractionation and its primitive nature. LB has a high Mg-number ranging between 0.60 and 0.63 with an average 0.62. For the purpose of Mg# calculations, the Fe_2O_3 is considered to equal to TiO_2 + 1.5 (Irvine and Barager, 1971). Wedephol (1975) and Wilson (1989) reported that a value of (Mg#) > 0.7 as a threshold that characterizes primitive magmas while Clague and Ferry (1982) suggested a value of 0.65 as distinction value. Moreover, the total Fe-content of LB, calculated as FeO, ranges between 11.92 and 12.99 wt% with average 12.38 wt%. It reflects that the rock is enriched in iron. Shaw et al. (2003) suggested that SiO_2 under saturated magma with a high MgO > 7 wt% and high FeO > 11 wt%. All these are evidences for a smaller degree of partial melting at high pressures (i.e. a deep-seated mantle source).

LB has Na_2O and K_2O averages of 3.42 and 0.65 wt%, respectively. The total Na_2O+K_2O values are very similar throughout the samples amounting to 4.72 wt% on average. The average value of Na_2O/K_2O ratio is 5.82, reflecting the sodic affinity of the rock (Figure 3). Furthermore, the Al_2O_3/ TiO_2 ratio average is 8.60 wt%, which indicates basic affinity of the rock.

4.2.2. Trace Elements

The Lb has relatively high Ni and Cr contents. Ni varies between 193 ppm and 271 ppm and averages 230 ppm. This may reflect that the LB has a limited olivine fractionation. Cr content ranges from 234 ppm to 374 ppm, and averages 313 ppm, with a Cr/Ni ratio about 0.074. The high content of Ni and Cr may also indicate that parental magma have been derived through partial melting of a peridotite mantle source (Wilson, 1989).

Rb content in LB is relatively low, ranging from 7 to 10 ppm and averages 8.8 ppm. This value is lower than the value of 22 ppm reported for alkali basalt by (Coleman and McGuire, 1988) and provides an argument against plagioclase fractionation. This was further supported by the high K/Rb ratio, which averages at 625. Sr content ranges from 505 to 727 with an average of 552.5 ppm. The LB has Zr content ranging from 102 to 108 ppm. Nb content ranges between 13 and 16 ppm. The average of Zr/Nb ratio is 7.5. The Y content is low and shows a very limited variation that ranges from 16 to 21 ppm, with an average Y/Nb ratio that equals 1.3. This ratio is consistent with the ratio of >1 reported by Pearce and Cann (1973) for the intra-continental alkali basalt.

5. Discussion and Conclusions

Several discriminatory diagrams were applied to help in the classification, nomenclature and interpretation of the tectonic setting of the LB. On the Midlemost et al. (1975) diagram, samples were plotted in the mildly alkali field (Figure 4). The Zr versus Y/Zr diagram of Pearce and

Norry (1979) illustrated the behavior of Zr and Y relative to the index of fractionation of three non-cumulate basalts settings. Here, LB samples fall within the intraplate basalt field with higher Zr/Y ratios than the MORB and Island Arc basalts (Figure 5).

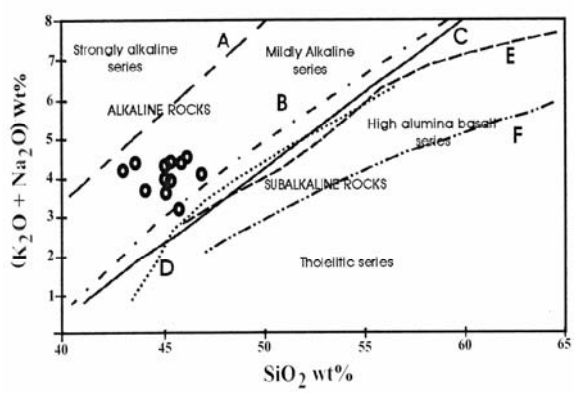

Figure 4: Total Alkali-silica diagram from LB. Dividers are A: Saggerson and Williams (1964), B: Irvine and Baragar (1971), C: Macdonald & Katsura (1964), D, E, F: Shwarzer & Roger (1974).

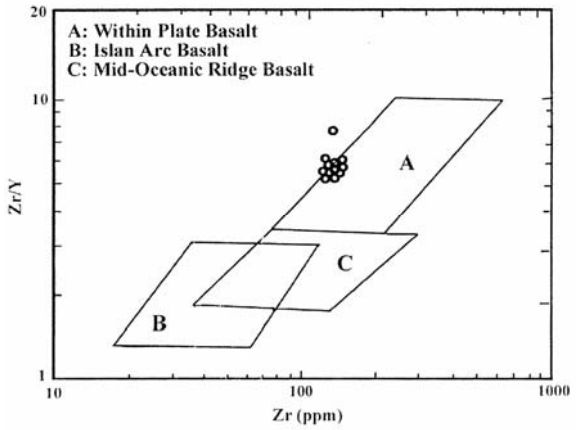

Figure 5: Zr-Zr/y diagram (Pearce & Norry, 1979) for the LB.

This is further supported by the ternary diagram of Pearce and Can (1973), which uses the Ti, Zr and Y to distinguish between island-arc tholeiites, MORB, calc-alkaline and intraplate basalts. On this diagram, all samples were plotted in the intraplate basalt field (Figure 6). Floyd and Winchester (1975) diagram is based on TiO_2 versus Y/Nb in order to distinguish between oceanic alkali basalt (OAB), continental alkali basalt (CAB), oceanic tholeiites (OTB) and continental tholeiites (CTB). LB samples fall on the CAB field (Figure 7) indicated also a continental intraplate tectonic setting. Moreover, the TAKTIP-diagram (K_2O/total alkali versus TiO_2/ P_2O_5 diagram) of (Chandrasekharam and Parthasarthym, 1978) is another helpful plot to discriminate intraplate basalt from rift volcanic. Here, LB samples fall in the field of rift volcanic (Figure 8).

One of the primary purposes of the present research is to study the kind of primitive nature of magma that gave rise to LB alkali olivine basalt. As mentioned previously, the low SiO_2 content (43.63 to 46.61 wt%), the high MgO content (mostly > 7 wt%) and the total FeO content (> 11 wt%) are distinctive criteria for the slightly fractionation nature of the LB. Moreover, they exhibit relatively high concentration of Cr (between 234 and 374 ppm) as compared to values reported for relatively primary magmas (e.g. Hughes, (1982), a value of 142 ppm, Al-Malabeh, (1994), a value of 185). This is also a good geochemical indicator for slightly clino-pyroxene fractionation of LB magmas.

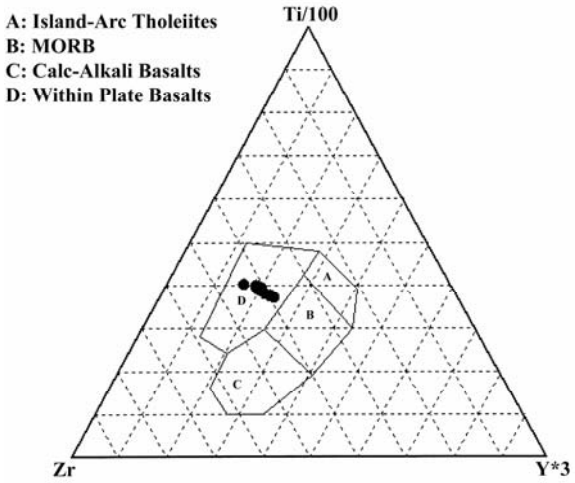

Figure 6: Ti-Zr-Y diagram (*Pearce & Can*, 1973) for the LB.

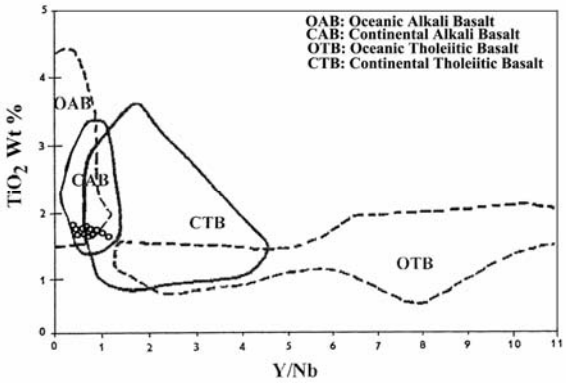

Figure 7: TiO2-Y/Nb diagram (*Floyd and Winchester*, 1975) for the LB.

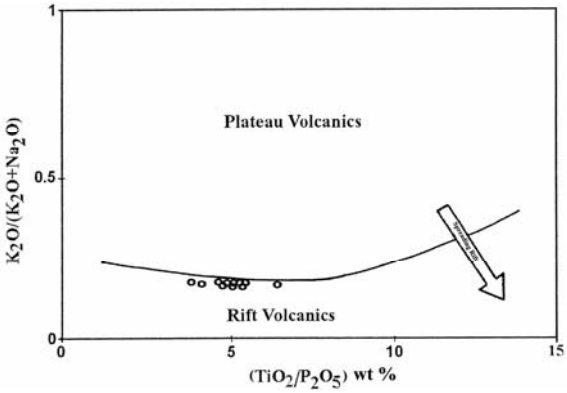

Figure 8: TAKTIP diagram-weight % K2O/total alkalies versus TiO2/P2O5 (*Chandasekharamand & Parthasarthy*, 1978), with arrow due to *Solyom et al*. (1985) for the LB.

Trace element ratios such as Ba/Rb, Rb/Sr, K/Ba and K/Rb and the low Rb content exclude magma mixing and crustal contamination, and provide an evidence for a primitive homogeneous source (Clague and Ferry, 1982); and Cebria and Lobez-Ruiz, 1995). This result is further supported by the Sr-Zr plot after (Camp and Roobol, 1992), where all samples fall into a partial melting trend rather than suggesting plagioclase

fractionation (Figure 9). However, the limited variation may reflect slight plagioclase fractionation.

The degree of ppartial melting is quantified by the non-modal batch melting equation of (Shaw, 1970) as follows:

$$C_l = C_o/D_o+F(1-P_i) \quad (1)$$

Where F is the melting degree, C_o and C_l are the concentrations of elements in the source and in the liquid, respectively. D_o and P_i are the bulk distribution coefficients of elements in the initial assemblage and for the minerals entering into the liquid, respectively. Using the mineral melt distribution coefficient model for Rb and Zr (Clague and Frey, 1982), these incompatible elements have very low D_o and P_i values, which are much smaller than the numerical values for partial melting (Camp and Roobol, 1989). In that case $C_l/C_o \approx 1/F$ and $F= C_o/C_l$., the F values are calculated using concentrations in a primordial mantle source (C_o) of 11.2 and 0.64ppm for Zr and Rb, respectively. Using these parameters, the studied samples give partial melting degrees averaging around 10% (Rollinson, 1993). These values compare well with the previous published studies for the Jordanian and Arabian intaplate basalt (e.g. Camp and Roobol, 1989; Shaw et al. 2003; Al-Malabeh et al. 2002).

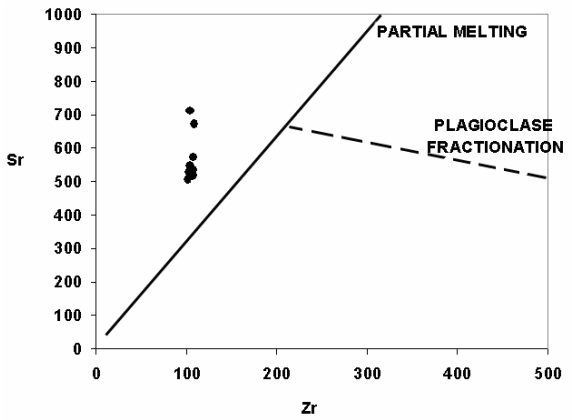

Figure 9: Plot of LB samples on Sr-Zr diagram (*Camp & Roobol,* 1989) showing the limited plagioclase fractionation.

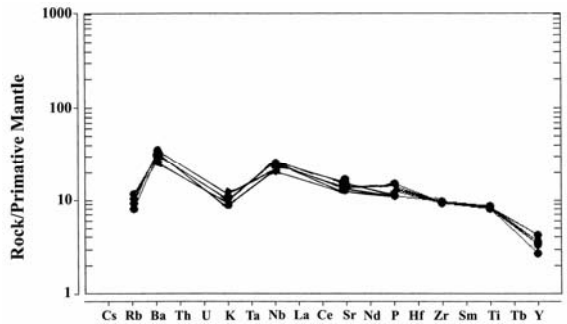

Figure 10: Spider diagram of incompatible elements from LB normalized to primitive mantle source. Elements are arranged in order of increasing incompatibility with mantle rocks.

Fundamental information regarding the nature of the inferred source origin can be obtained based on the homogeneity of the major oxides and trace elements patterns that suggest that LB is most likely to be a result of partial melting of a relatively homogeneous mantle source. This is further supported by trace elements ratios such as K/Ba, Ba/Rb and Zr/Nb (Peltz and Bratosin, 1986). As well the low and consistent Y content, the high Zr/Y and the TiO_2/Y ratios (Frey and Roy, 1978; and Downes et al. 1995) indicate that the sources are garnet rather than spinel bearing rocks. The normalized trace elements spider diagram of the rock/primitive mantle shows a positive Nb peak, which is a good indicator that LB is a product of the asthenospheric part of the mantle rather than the lithospheric part (Thompson, 1986; and Wilson, 1989) (Figure 10).

Acknowledgment

The authors would like to express their deep thanks to the staff of Geological Institute, University of Wuerzburg/Germany, for their help in analytical procedures. Also thanks are due to Prof. Dr. S. Kembe, University of Darmstadt / Germany for his valuable reviewing of the manuscript.

References

[1] Al-Malabeh, A., 2003. Geochemistry and Volcanology of Jabal Al-Rufiyat, Strombolian Monogenic Volcano, Jordan, Dirasat, 30: 125-140.

[2] Al-Malabeh, A., Al-Fugha, H., and El-Hasan, T., 2004. Petrology and Geochemistry of Late Precambrian magmatic rocks from southern Jordan, N. JB. Palaent. Abh., 233 (3): 333-350.

[3] Al-Malabeh, A., 1993. The volcanology, mineralogy and geochemistry of selected pyroclastic cones from NE-Jordan and their evaluation for possible industrial applications, Ph.D. thesis, Erlangen University, Germany.

[4] Al-Malabeh, A., 1994. Geochemistry of two volcanic cones from the intra-continental plateau basalt of Harra El-Jabban, NE-Jordan, Geochemical Journal, 28:517-540.

[5] Al-Malabeh, A., El-Hasan, T., Lataifeh, M., and O'Shea, M., 2002. Geochemical- and Mineralogical-Related Magnetic Characteristics of the Tertiary-Quaternary (Umm A-Qutein) Basaltic Flows from the Basaltic Field of Harra El-Jabban, Northeast Jordan, Physica B-Physics of Condensed Matter, Netherlands. 321 (1-4): 396-403.

[6] Almond, D.C., 1986. The relation of Mesozoic magmatic volcanicity to tectonics in the Afro-Arabian Dome, J. Volcanol. Geotherm Res., 28: 225-246.

[7] Al-Shawabkeh, K., 1991. The geology of the Adir area. Unpublished report, NRA, Jordan.

[8] Barberi, F., Borsi, S., Ferra, G., Marinelli, G., & Vareet, J., 1970. Relations between tectonics and magmatology in the northern Dankil depression (Ethiopia). Philos. Trans. R. Soc, London, 267: 293-311.

[9] Barberi, F., Capaldi, G., Gasperini, P., Marinelli, G., Santacroce, R., Scandone, R., Treuil, M., Varet, J., 1979. Recent basaltic volcanism of Jordan and its implications on the geodynamic evolution of the Afro-Arabian rift system, Academia Nazionale Dei Lincei, Att Del Convegni Lincei, 47, Rome, 667-83.

[10] Barjous, M., and Mikbel, S., 1990. Tectonic evolution of the Gulf of Aqaba-Dea Sea transform fault. In: R. Kovach and Z. Ben Avraham (Eds.) Geologic and tectonic processes of the Dead Sea Rift zone, Tectonophysics, 180: 49-59.

[11] Bender, F. (1974): Geology of the Arabian peninsula, Jordan. US Geol. Surv. Prof. Paper, 560-1, 36 p.

[12] Bentor, Y., 1985. The crustal evolution of the Arabo-Nubian massif with special reference to the Sinai Penisula, Precambr. Res., 28: 1-74.

[13] Burke, K., 1996. The African plate, South African Journal of Geology, 99: 341-409.
[14] Camp, V., & Roobol, M., 1992. Upwelling asthenosphere beneath western Arabia and its regional implications, Journal of Geophysical Research, 97: 15255-15271.
[15] Camp, V., Roobol, M., 1989. The Arabian continental alkali province: Part I Evolution of Harrat Rahat, Kingdom of Saudi Arabia, Geological Society of. America Bulletin, 101: 71-95.
[16] Cebria, J.; and Lopez-Ruiz, J., 1995. Alkali basalt and leucitites in an extentional Intra plate setting: The Late Cenozoic Calatrava volcanic province (Central Spain), Lothos, 35: 27-46.
[17] Chandrasekhram, D., and Parthasarthy, A., 1978. Geochemical and tectonic studies on the coastal and inland Deccan Trap volcanics and a model for the evolution of Deccan Trap volcanism, N. JB. Mineral. Abh., 132:128-145.
[18] Clague, D., Frey, F., 1982. Petrology and trace elements geochemistry of Honolulu volcanism: Implications for the ocean mantle below Hawaii, Journal of Petrology, 23: 447-504.
[19] Coleman, R., and McGuire, A., 1988. Magma systems related to the Red Sea opening, Tectonophysics, 150:77 –100.
[20] Cox, K., Bell, J., and Pankhurst, R., 1979. The interpretation of igneous rocks, 4th in press., London.
[21] Downes, H., and Seghedi, I., Szakacs, A., Dobosi, G., James, D., Vaselli, O., Rigby, I., Ingram, G., Rex., D. and Peckskay, Z., 1995. Petrology and geochemistry of Late Tertiary/Quarernay mafic alkali volcanism in Romania, Lithos, 35: 65-81.
[22] Duffield, W. Mc Kee, E., El Salem, F., Feimeh, M., 1988. K-Ar ages, chemical composition and geothermal significance of Cenozoic basalt near the Jordan Rift, Geothermics, 17: 635-644.
[23] Floyd, P., and Winchester, J., 1975. Magma type and tectonic setting discrimination using immobile elements. Earth and Planetary discrimination using immobile elements, Earth and Planetary science letters, 27: 211-218.
[24] Frey, F., Green, D. and Roy, S., 1978. Integrated models of Basalt Petrogenesis: A study of Quartz tholeiites to olivine melilites from South Eastern Australia utilizing geochemical and experimental petrological data, J. Petrol., 19: 463 – 513.
[25] Garfunkel, Z., 1988. Relation between continental rifting anduplifting: evidence from Suez rift and northern Red Sea, Tectonophysics, 150: 33-49.
[26] Garfunkel, Z., 1989. Tectonic setting of Phanerozoic magmatism in Israel, Isr. J. Earth Sci., 38: 51-74.
[27] Hatcher, R. Zietz, I., Regan, R. and Abu-Ajammieh, M., 1981. Sinistral strike-slip motion on the Dead Sea rift: confirmation from new magnetic data, Geology, 9: 458-462
[28] Heimbach, W., and Huseibeh, M., 1975. The geological and hydrogeological surveys in the area between the Hejaz Railway Qatrana-El Hasa and the eatern border of Jordan, Unpublished report and maps, NRA, Jordan.
[29] Hughes, C., 1982. Igneous petrology. Development in petrology. Elsevier, New York.
[30] Ibrahim, K. (1996): The regional geology of Al-Azraq area. NRA. Geol. Dir. Map Div. Bull. 36, P 67.
[31] Ibrahim, K., and Al-Malabeh, A., 2006. Geochemistry and Volcanic Features of Harrat El Fahda, A young Volcanic Field in Northwest Arabia, Jordan. Journal of Asian Sciences. 127(2):127-154.
[32] Ilani, S., Harlavan, Y., Tarawneh, K., Rabba, I., Weinberger, R., Ibrahim, K.M., Peltz, S;. and Steinitz, G., 2001. New K-Ar ages of basalts from the Harrat Ash Shaam volcanic field in Jordan: implications for the span and duration of the upper mantle upwelling beneath the western Arabian plate, Geology, 29: 171-174.
[33] Irvine, T., and Barager, W., 1971. A guide to the chemical classification of the common rocks, Canadian Journal of Earth Science, 8: 523-548.
[34] Jenner, G., Gawood, P., Rautenschlein, M. and White, W., 1987. Composition of back-arc basin volcanics, Valufa ridge, Lau basin: evidence for a slab-derived component in their mantle source, J. Volcanol. Geotherm. Res., 32: 209-222.
[35] Kerr, P. (1977): Optical Mineralogy. John Wiley and Sons, New York.
[36] Lataifeh, M., Al-Malabeh, A. and El-Hasan, T., 2002. Geochemical and Magnetic Investigations of El-Lajjoun Cenozoic Basaltic Rocks, Central Jordan, Abhath Al-Yarmouk, 11: 337-347.
[37] Le Bas, M.J., Le Maitre, R.W., Streckeisen, A., Zanettin, B., 1986. A chemical classification of volcanic rocks based on the total alkalis-silica diagram, Journal of Petrology, 27: 745-750.
[38] Macdonald, G., and Katsura, T., 1964. Chemical composition of Hawaiian lavas, J. Petrol., 5: 82-133.
[39] Middlemost, E., 1975. The basalt Clan., Earth Sci. Rev., 11: 337 – 564.
[40] Moffat, D., 1988. A volcanotectonic analysis of the Cenozoic continental basalts of northern Jordan: implications for hydrocarbon prospectively in the block B area, Unpubl. Report. University college of Swansen, Uk.
[41] Pearce, J., and Cann, J. R,. 1973. Tectonic setting of basic volcanic rocks determined using trace element analysis, Earth Planet Sci. Lett., 19: 290-300.
[42] Pearce, J., and Norry, M., 1979. Petrogenetic implications of Ti, Zr, Y, and Nb variations in volcanic rocks, Contributions to Mineralogy and Petrology, 69(1): 33-47.
[43] Peltz, S., and Bratosin, W., 1986. New data on the geochemistry of the Quaternary basalts in Pensani mountains, D.S, Inst. Geol. Geofiz., 71: 389-403.
[44] Pick, R., Deniel, C., Coulon, C. Yirgu, G. and Marty, B., 1999. Isotopic and trace element signatures of Ethiopian flood basalts: evidence for plume-lithosphere interactions, Geochimica et Cosmo-chimica Acta, 63: 2263-2279.
[45] Saffarini, G, Nassir, S., and Abed, A., 1985. A contribution to the petrology and geochemistry of the Quaternary-Neogene basalts of central Jordan, Dirasat, 12: 133-144.
[46] Schwarzer R., and Rogers, J., 1974.A worldwide comparison of alkali olivine basalts and their differentiation trends, Earth Plant. Sci. Lett., 23: 286-296.
[47] Shaw, D.M., 1970. Development of the early continental crust, Part I. Use of trace elements distribution coefficient model for the proto-Archean crust, Can. J. Earth. Sci., 9: 1577-1595.
[48] Shaw, J., Baker, J., Menzies, M., Thirlwall, B., and Ibrahim, K., 2003. Petrogensis of the largest intraplate volcanic field on the Arabian plate (Jordan): a mixed lithosphere-asthenosphere source activated by lithosphere extension, J. Petrol., 44(9): 1657-1679.
[49] Solyom, Z., Andreasson, P. Johansson, I., 1985. Petrochemistry of Late Proerozoic rift volcanism in Scandinavia, mafic dike swarms in constructive and abortive arms, Intr. Conf. on Mafic Dyke Swarms, Uni. Toronto Reindale Campus, Ont., Abstract book, Vol., p. 164-171.
[50] Steinitz, G., and Bartov, Y., 1992. The Miocene-Pleistocene history of the Dead Sea segment of the Rift in light of K-Ar ages of basalts, Isr. J. Earth Sci., 40: 199-208.
[51] Stern, R., 1985. The Najed fault system, Saudi Arabia and Egypt. A late Precambrian rift system, Tectonics,. 4: 497-511.
[52] Thompson, R., 1986. Sources of basic magmas. Nature, 319: 448 – 449.
[53] Rollinson, H., 1993. Using Geochemical Data: Evaluation, Presentation, Interpretation. Longman Scientific & Technical, Essex, pp352.

[54] Wilson, M., 1989. Igneous petrogenesis, a global tectonic approach. Unwin Hyman, London.